02,07

Superconducting Tm123 granules on non-superconducting Pr123 seeds

© D.M. Gokhfeld, S.V. Semenov, I.V. Nemtsev, M.I. Petrov

Kirensky Institute of Physics, Federal Research Center „Krasnoyarsk Scientific Center,
Siberian Branch, Russian Academy of Sciences“,
Krasnoyarsk, Russia

E-mail: gokhfeld@iph.krasn.ru

Received June 25, 2025
Revised June 25, 2025
Accepted June 28, 2025

Annealing of a two-component mixture of metal oxide powders with the same crystal structure, but different peritectic temperatures, can lead to accelerated growth of granules of the low-melting phase. This paper describes the preparation and investigation of the microstructural and magnetic characteristics of large grain ceramics in which $PrBa_2Cu_3O_{7-\delta}$ (Pr123) is a refractory component, and $TmBa_2Cu_3O_{7-\delta}$ (Tm123) is a component with a lower peritectic temperature. In a compound prepared from 80 vol.% Tm123 and 20 vol.% Pr123, the size of superconducting Tm123 granules reaches 0.1 mm. The presence of large granules leads to high values of remanence magnetization and trapped magnetic flux. Despite the presence of 20 % of the non-superconducting phase, the remanence magnetization in the resulting compound is only 1.07 times less than in the related large grain ceramics of 80 vol.% Tm123 and 20 vol.% Nd123, and exceeds the values of the remanence magnetization in polycrystalline superconductors obtained by standard solid-phase synthesis.

Keywords: High-Tc superconductors, magnetic hysteresis, magnetization, REBCO, solid state synthesis, trapped magnetic flux.

DOI: 10.61011/PSS.2025.07.61867.169-25

1. Introduction

The progress in the development of superconducting bulk materials and superconducting tapes opened the paths towards wide application of superconductors in high current devices for generation of strong magnetic fields and energy transfer. Today the main used high-temperature superconductors (HTSC) — are $RE\ Ba_2Cu_3O_{7-\delta}$, where RE — is a rare earth element. The main methods of industrial production of HTSC — are the creation of single-domain samples by the method of growth on the seed from the melt [1] and production of flexible tapes by laser sputtering on different substrates [2]. However, the considerable quantity of the exploratory works to produce new superconductors, to optimize conditions of synthesis, to modify composition, to introduce nanoparticles, to create nanoscale materials are carried out in ceramic materials [3–10]. To prepare such polycrystalline superconducting materials, they use solid phase synthesis [11] and sol gel method [12], which differ by relative simplicity and wide opportunities of microstructure modifications of the produced superconductors. Development of the affordable synthesis methods is necessary to optimize the properties of the known materials and to search for the new superconductors [13].

The necessary stage in the synthesis of ceramic high-temperature superconductors is the high-temperature annealing, which forms a superconducting orthorhombic phase. Annealing parameters, for example, temperature and duration, impact the critical temperature, critical current density, material strength. Through variation of the annealing condition and selection of the annealed mixture components it is possible to control the thickness and the conductivity of the intergranular boundaries [14–18], to control the size of the granules [19–22] and to obtain the new phases at the boundaries of precursor phases [23–25]. Such control of the material morphology is used to develop the ceramic cuprate superconductors and may turn out to be successful for other classes of superconducting compounds.

In recent papers [26,27] we demonstrated that at high temperature annealing of the mixture of polycrystalline materials $NdBa_2Cu_3O_{7-\delta}$ (Nd123) and $TmBa_2Cu_3O_{7-\delta}$ (Tm123) with differing peritectic temperatures, the superconducting granules may rise to 0.1 mm. The mixture annealing temperature is selected as higher or equal to the peritectic temperature of the low-melting phase, but lower than the peritectic temperature of the hard-melting phase. For growth of granules upon annealing of the two-component mix, the peritectic temperatures of components must differ by dozens of degrees. Peritectic temperatures of the compounds RE123 discussed in the paper are given in the table [1,28]. Heating of the rare earth element mix to the peritectic temperature of the low-melting component leads to its disintegration to create a liquid phase. Large granules grow from the liquid phase in hard-melting crystallite seeds. The similar process of the crystal growth in the hard-melting seed from the liquid phase is implemented in the known method of top-seeded melt growth [29]. However, the top-seeded melt growth is complicated, requires expensive equipment and takes time. The samples grown by this method contain cracks, pores and inhomogeneities related to

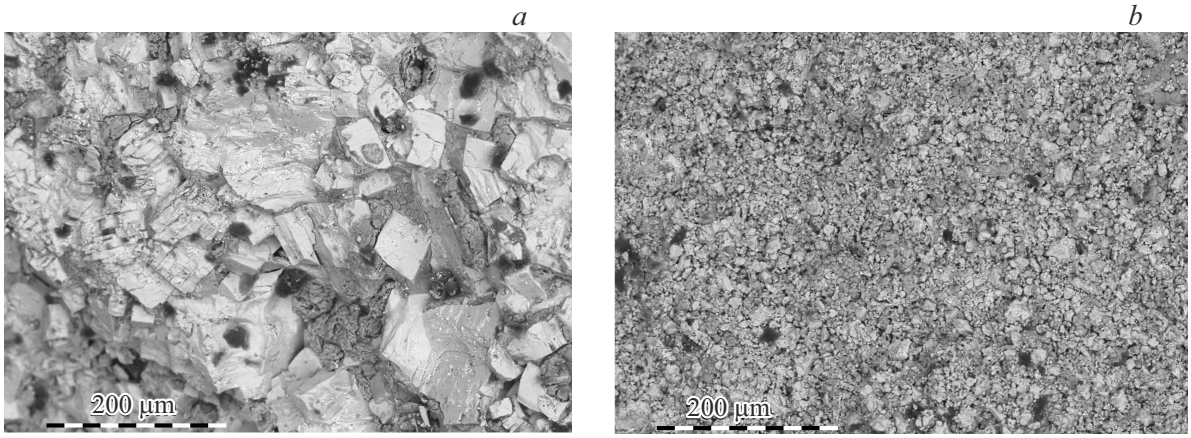

Figure 1. Granules in (a) Tm(Pr)123 and (b) Tm123.

Peritectic temperatures of some compounds $RE123$

RE in $RE123$	Peritectic temperature, °C
Pr	1052
Nd	1068
Tm	980

uneven saturation with oxygen [30]. The method to produce polycrystalline superconductors from the two-component mix maintains the simplicity of the solid phase synthesis, is not demanding to the equipment and makes it possible to produce high quality granules.

In the presented paper the described method is used to create a large-granule superconductor as proposed in [26,27]. The hard-melting precursor is $PrBa_2Cu_3O_{7-\delta}$ (Pr123). The low-melting precursor and concentrations of components are selected the same as in [26,27], so that it is possible to compare them to the previous results. Pr123 stands out from the series $RE123$ by not transitioning to the superconducting state. Because Pr123 is used, the non-superconducting inclusions arise in the synthesized material. The conducted measurements of magnetization and the comparison to the results of the magnetic measurements of the large-granule superconductor synthesized from the superconducting precursors Nd123 and Tm123, made it possible to establish how large granules and non-superconducting inclusions impact the magnetic flux trapping.

2. Experiment

Polycrystalline materials $PrBa_2Cu_3O_{7-\delta}$ (Pr123) and $TmBa_2Cu_3O_{7-\delta}$ (Tm123) were produced from powders Pr_2O_3, Tm_2O_3, $BaCO_3$ and CuO using the standard ceramic technology of solid phase synthesis. The cycle consisting of grinding, pressing, annealing at 910 °C and cooling with a furnace was repeated three times. The finished ceramic materials were ground and mixed at the proportion of 20 vol.% Pr123 and 80 vol.% Tm123. The mix was pressed, the produced pellets were annealed at 980 °C for 1 hour and cooled with the speed of 0.5 °C per minute. Further the designation Tm(Pr)123 is used for the synthesized material.

The measurements were carried out using the equipment provided by the Krasnoyarsk Regional Center of Research Equipment of Federal Research Center Krasnoyarsk Scientific Center, Siberian Branch of the Russian Academy of Sciences. The microstructure characterization of the samples was carried out using the scanning electron microscope Hitachi TM4000Plus and energy-dispersive spectrometer Bruker XFlash 630Hc. Magnetization was measured using a vibration magnetometer Quantum Design PPMS-9T. The sample for the magnetic measurements had the shape of the parallelepiped $5 \times 2 \times 1.5$ mm. The magnetic field was directed along the long side of the sample.

3. Results and discussion

Images in Figure 1, a, produced using the scanning electron microscopy, demonstrate the enlarged granules in Tm(Pr)123 compared to the initial polycrystalline material Tm123 (Figure 1, b). The size of the largest granules reaches 0.1 mm.

Energy-dispersive spectrometry shows heterogeneous distribution of Tm and Pr on the surface of the samples (Figure 2). Thulium is present mostly in the large granules (with dimensions from 5 μm to 100 μm).

Temperature of the superconducting transition T_c was defined as value T, when magnetization becomes positive being heated from low temperatures (see insert in Figure 3). The obtained value $T_c = 91.8 \pm 0.2$ K matches T_c of Tm123 [26]. Magnetic hysteresis loops of Tm(Pr)123 measured at $T = 4.2$, 30, 60, 80, 100 K, are given in Figure 3. Loops have an inclination caused by paramagnetic

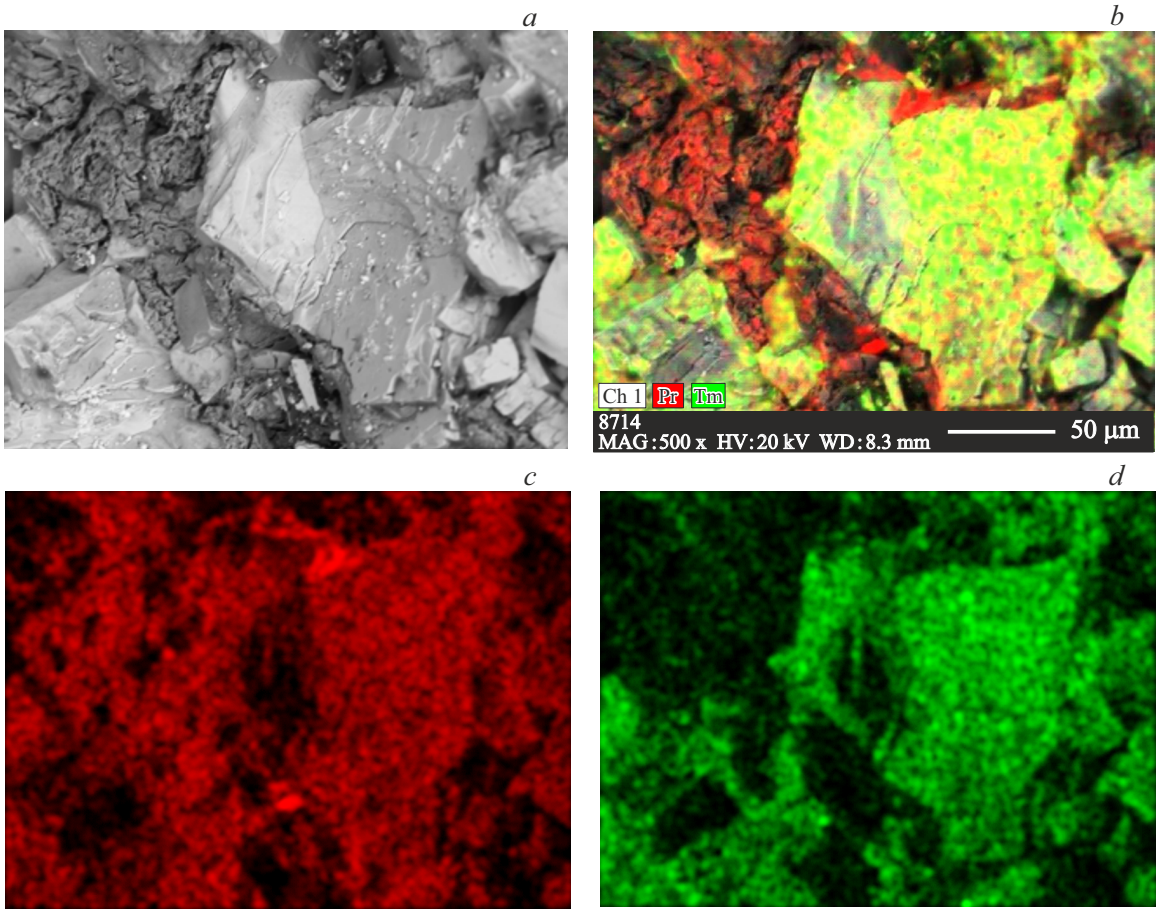

Figure 2. Distribution of chemical elements on the surface of Tm(Pr)123.

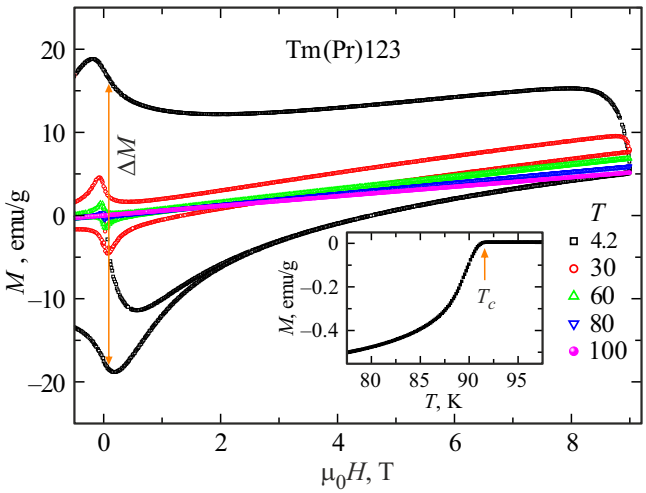

Figure 3. Tm(Pr)123 magnetic hysteresis loops. The insert shows the dependence of magnetization on the temperature in the field of 100 Oe, measured after zero-field cooling (ZFC).

contribution from rare-earth ions. The appearance of the magnetic hysteresis loops is typical for the polycrystalline HTSC.

To determine the impact of the non-superconducting granules Pr123 at the superconducting properties of Tm(Pr)123, the comparison was done to the large-granule material Tm(Nd)123, consisting of superconducting granules of two grades (80 vol.% Tm123 and 20 vol.% Nd123) [26,27].

Figure 4, *a*, *b* shows the magnetic hysteresis loops of samples Tm(Pr)123 and Tm(Nd)123. To compare the superconducting samples, it is convenient to consider the values ΔM, the difference between the magnetization values with the decrease and increase of the external magnetic field H (see Figure 3). Value $\Delta M(H, T)$ for the polycrystalline superconductor depends on the density of the intragranular critical current $J_c(H, T)$, the granule size and the proportion of the superconducting phase in the sample [31,32]. Let us assume that the intragranular density of the current and the averaged dimensions of granules Tm123 for these samples differ insignificantly since Tm(Pr)123 and Tm(Nd)123 were synthesized using the same technology. Then the decrease in the proportion of the superconducting granules from 100 % to 80 % must result in the decrease of value $\Delta M(H)$ 1.25 times. As the magnetic hysteresis loops demonstrate at $T = 4.2$ K (Figure 4, *a*), values $\Delta M(H)$ are ≈ 1.33 times lower for Tm(Pr)123 than

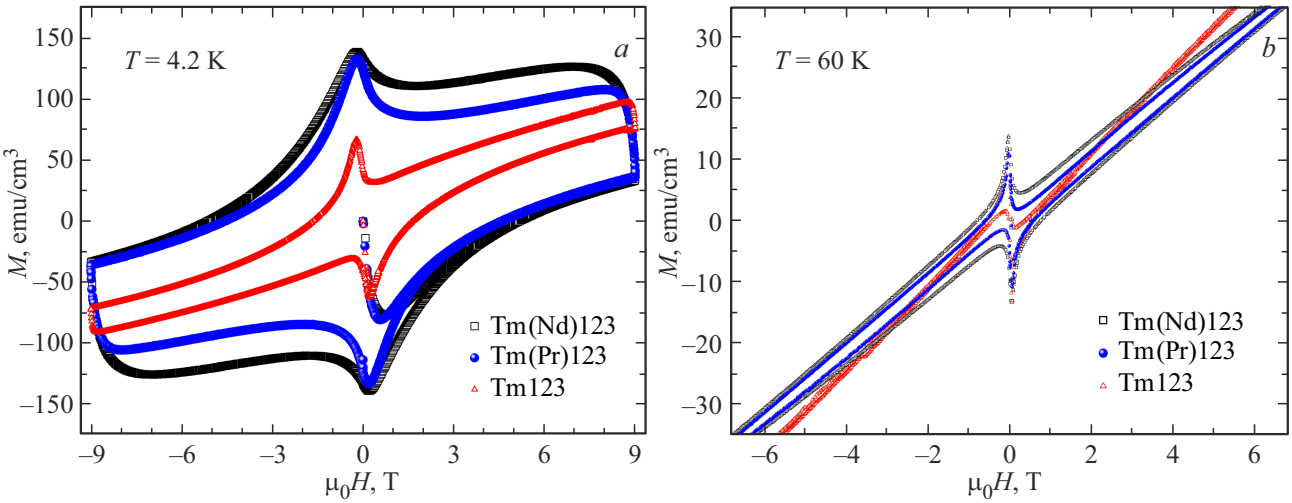

Figure 4. Magnetic hysteresis loops of large-granule samples Tm(Nd)123 and Tm(Pr)123 and polycrystalline Tm123 at $T = 4.2$ K and $T = 60$ K.

for Tm(Nd)123 at $H \geq 1$ T. Therefore, the decrease of ΔM corresponds to the decrease in the proportion of the superconducting phase when non-superconducting seed granules are used instead of superconducting ones. Note that the actual proportions of the superconducting phase in the samples of Tm(Pr)123 and Tm(Nd)123 may be less than 80 % and 100 %.

The critical current density J_c was calculated from the magnetization loops using formula $J_c = 3\Delta M/d$, here d — is the effective scale of current circulation. This paper defined d using the method proposed in paper [33]. The method is based on the fact that Abrikosov vortices are not fixed in the near-surface layer of the superconductor with the thickness equal to the depth of magnetic field penetration λ. Equilibrium magnetization of the near-surface layer causes asymmetry of magnetization: the magnetization values at the increase of the field M^+ are higher by module than the values of magnetization at the decrease of the field M^- (without a paramagnetic contribution). The observed asymmetry of the magnetic hysteresis loop makes it possible to define the current circulation scale: $d \approx 2\lambda/[1 - (\Delta M/2|M_m^-|)]$ higher indices, where M_m^- — minimum value of magnetization, i.e. the maximum value of the diamagnetic signal, $\lambda = 150 \cdot 10^{-9}$ m. Using this method for the magnetic hysteresis loop at $T = 4.2$ K, we get the value $d \approx 10\,\mu$m.

The estimated dependences J_c on the magnetic field at different temperatures are shown in Figure 5, *a*. Since the main contribution to magnetization is provided by the superconducting granules, the values ΔM for Tm(Pr)123 when calculated using (1) were additionally divided by the proportion of phase Tm123 at $T = 4.2$ K. Under such approach, the calculated values of the intragranular density of critical current do not depend on the proportion of the non-superconducting phase. The decrease of the proportion of the superconducting phase with the temperature was not taken into account.

When the temperature increases, the critical current density J_c decreases, and ΔM decreases accordingly. However, for Tm(Pr)123 the decrease of ΔM happens faster than for Tm(Nd)123. At $T = 60$ K the values $\Delta M(H)$ for Tm(Pr)123 are lower than for Tm(Nd)123, 2 times (Figure 4, *b*), and at $T = 80$ K — 2.5 times (the magnetic hysteresis loops at $T = 80$ K are not provided). Such decrease in the values of ΔM that accelerates with the temperature may be caused by the presence of the phases with the lower critical temperature. It is known that the partial substitution of the position *RE* for Pr in the superconducting *RE*123 causes the suppression of superconductivity and decrease of T_c [34]. We assume that in the interfaces of Tm123 and Pr123 the synthesis led to diffusion of Tm and Pr to form mixed phases $Tm_{1-x}Pr_xBa_2Cu_3O_{7-\delta}$ with $0 < x < 1$. Seemingly, at $T = 4.2$ K not more than 80 % of the Tm(Pr)123 volume is in the superconducting state, and at temperature increase the proportion of the material in the superconducting state decreases, making only around 50 % at $T = 60$ K and 40 % at $T = 80$ K. Therefore, the decrease in the proportion of the superconducting phase in Tm(Pr)123 impacts the speed of decrease of ΔM with the temperature increase.

Dependences of the pinning force density $F_p(H)$ calculated using formula $F_p(H) = \mu_0 H \cdot J_c(H)$ are given in Figure 5, *b*. Dependences of $F_p(H)$ at $T = 60$ K and $T = 80$ K have the maximum at 5.3 T and 1.1 T accordingly. The same values of the maximum field H_{max} at 60 K and 80 K had the dependences $F_p(H)$ of the Tm(Nd)123 sample [27]. A dimensionless parameter $h_{max} = H_{max}/H_{irr}$, where H_{irr} — is the irreversibility field, is related to the pinning features [35]. For Tm(Nd)123 and Tm(Pr)123 $h_{max} \approx 0.2$. According to the scaling model [35], the value $h_{max} = 0.2$ corresponds to the pinning at intergranular boundaries. The same values

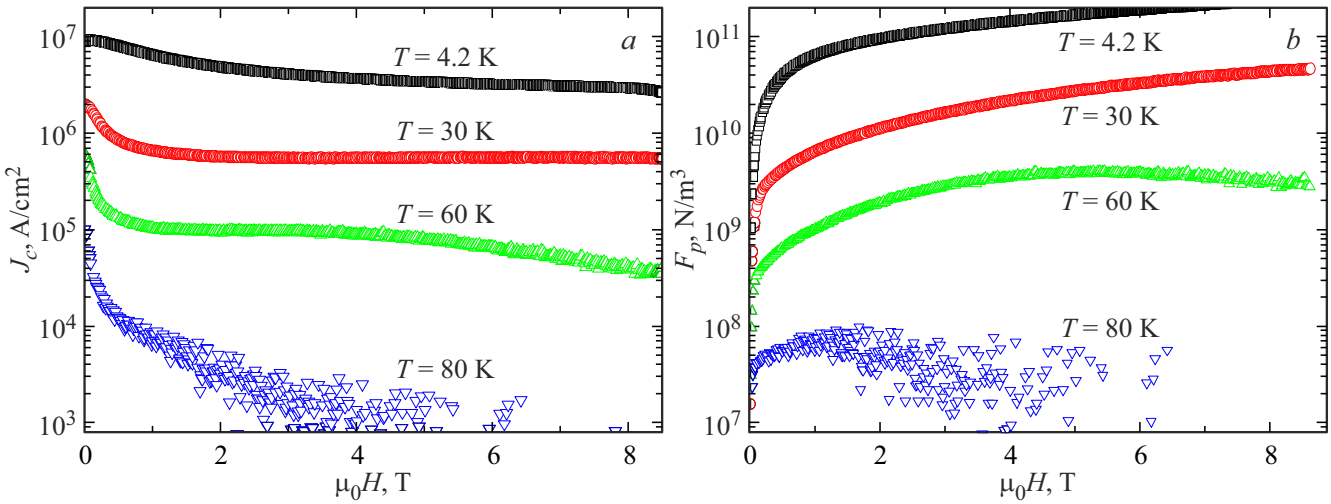

Figure 5. Dependences (*a*) of critical current density and (*b*) pinning force density on the magnetic field for Tm(Pr)123 (in semilogarithmic scale), calculated from the magnetic hysteresis loops.

of H_{max} and h_{max} for Tm(Nd)123 and Tm(Pr)123 indicate the same mechanisms of magnetic flux pinning in these superconductors.

The values of the remanence magnetization $M_{rem} = \Delta M(H = 0)/2$ of the studied sample considerably exceed M_{rem} of polycrystalline superconductors produced by the standard solid phase synthesis (see Figure 4, *a*, *b*, where the polycrystalline Tm123 loop is given for comparison). The trapped magnetic field B_{tr} and the trapped magnetic flux Φ are expressed as $B_{tr} = \mu_0 M_{rem}$ and $\Phi = \mu_0 M_{rem} S$, where S — is the surface area of the sample cross section with the plane perpendicular to the external field. The trapped magnetic field for Tm(Pr)123 is 0.155 T at $T = 4.2$ K, and the trapped magnetic flux is $4.7 \cdot 10^{-7}$ Wb. In the superconductors *RE*123, produced using the standard ceramic technology, the typical values of the trapped field do not exceed 0.1 T [36–38]. High values ΔM, M_{rem} and B_{tr} for Tm(Pr)123, as well as for Tm(Nd)123, are related to the larger size of the superconducting granules as $\Delta M \sim J_c d$.

Even though the content of the superconducting phase in Tm(Pr)123 and Tm(Nd)123 differs by 20 %, the values M_{rem} and B_{tr} for Tm(Pr)123 at $T = 4.2$ K is only less by 7 %. The abnormally small reduction of M_{rem} and ΔM in the weak fields for Tm(Pr)123 compared to Tm(Nd)123 may be caused by the trapping of the magnetic flux with the non-superconducting inclusions. It is more beneficial from the energy point of view for the magnetic flux to pass through the microscopic defects (pores, inclusions of the non-superconducting phase), and these defects serve as the centers of pinning [39–41]. However, such defects decrease the effective cross section for current flow, and the excessive trapping of the magnetic flux with the microscopic non-superconducting inclusions is only possible in the weak fields [42].

4. Conclusion

The high-temperature annealing of precursors with different peritectic temperatures (Tm123 and Pr123) is applied to produce the ceramic material with the large superconducting granules with the size of up to 0.1 mm. The granules were grown at the annealing temperature equal to the peritectic temperature of the low-melting component (Tm123).

Energy-dispersive spectrometry and comparison of ΔM values for the samples with the non-superconducting and superconducting nuclear granules show that in Tm(Pr)123 the large Tm123 granules are formed. Quick decrease of ΔM with temperature is explained by the formation of the mixed phase $Tm_{1-x}Pr_xBa_2Cu_3O_{7-\delta}$ with the lower critical temperature. Tm(Pr)123 material that contains 20 vol.% of non-superconducting Pr123, may trap the magnetic field of up to 0.155 T per 4.2 K, which is only 7 % lower than for Tm(Nd)123, and considerably exceeds the values B_{tr} for most polycrystalline superconductors.

Funding

The study was performed under the state assignment of the Institute of Physics, Siberian Branch of RAS.

Conflict of interest

The authors declare no conflict of interest.

References

[1] D.K. Namburi, Y. Shi, D.A. Cardwell. Supercond. Sci. Technol. **34**, 053002 (2021).
[2] K. Tsuchiya, X. Wang, S. Fujita, A. Ichinose, K. Yamada, A. Terashima, A. Kikuchi. Supercond. Sci. Technol. **34**, 105005 (2021).

[3] I.B. Bobylev, S.V. Naumov, N.A. Zyuzeva, S.V. Telegin. Phys. Met. Metallogr. **119**, 1175 (2018).
[4] N.A. Khalid, M.M. Awang Kechik, N.A. Baharuddin, C.S. Kien, H. Baqiah, L.K. Pah, A.H. Shaari, Z.A. Talib, A. Hashim, M. Murakami. J. Mater. Sci. Mater. Electron. **31**, 16983 (2020).
[5] P. Pęczkowski, P. Zachariasz, M. Kowalik, W. Tokarz, S.P. Kumar Naik, J. Żukrowski, C. Jastrzębski, L.J. Dadiel, W. Tabiś, Ł. Gondek. J. Eur. Ceram. Soc. **41**, 7085 (2021).
[6] S.K. Gadzhimagomedov, D.K. Palchaev, Z.K. Murlieva, M.K. Rabadanov, M.Y. Presnyakov, E.V. Yastremsky, N.S. Shabanov, R.M. Emirov, A.E. Rabadanova, J. Phys. Chem. Solids **168**, 110811 (2022).
[7] A.N. Kamarudin, M.M.A. Kechik, S.N. Abdullah, H. Baqiah, S.K. Chen, M.K.A. Karim, A. Ramli, K.P. Lim, A.H. Shaari, M. Miryala. Coatings **2022**, 12, 91 (2022).
[8] C. Min Cheong, S. Kien Chen. Mater. Today Proc. **96**, 50 (2024).
[9] K.S. Pigalskiy, A.A. Vishnev, N.N. Efimov, A.V. Shabatin, L.I. Trakhtenberg. Ceram. Int. **51**, 11037 (2025).
[10] R.A.M. Arebat, M.M.A. Kechik, H. Baqiah, C.S. Kien, L.K. Pah, K.K.M. Shariff, A.H. Shaari, Y.S. Hong, N.A.M.I.A. Sah, M. Miryala. J. Aust. Ceram. Soc. **1** (2025).
[11] M. Aykol, J.H. Montoya, J. Hummelshøj. J. Am. Chem. Soc. **143**, 9244 (2021).
[12] T.T. Thuy, S. Hoste, G.G. Herman, K. De Buysser, P. Lommens, J. Feys, D. Vandeput, I. Van Driessche. J. Sol-Gel Sci. Technol. **52**, 124 (2009).
[13] J.R. Chamorro, T.M. McQueen. Acc. Chem. Res. **51**, 2918 (2018).
[14] P.E. Kazin, V.V. Poltavets, Y.D. Tretyakov, M. Jansen, B. Freitag, W. Mader. Phys. C Supercond. **280**, 253 (1997).
[15] K.A. Shaihutdinov, D.A. Balaev, D.M. Gokhfeld, S.I. Popkov, M.I. Petrov. J. Low Temp. Phys. **130**, 347 (2003).
[16] D.A. Balaev, A.G. Prus, K.A. Shaykhutdinov, D.M. Gokhfeld, M.I. Petrov. Supercond. Sci. Technol. 20, 495 (2007).
[17] B.A. Malik, M.A. Malik, K. Asokan. Curr. Appl. Phys. **16**, 1270 (2016).
[18] D.S. Novosilova, M.V. Polikarpova, I.M. Abdyukhanov, I.L. Deryagina, E.N. Popova, E.I. Patrakov, A.S. Tsapleva, M.V. Alekseev. Phys. Met. Metallogr. **122**, 33 (2021).
[19] J.-Y. Kim, S.-Y. Lee, I.-S. Yang, T. Lee, S. Yom, K. Kim, J.H. Kim. Phys. C Supercond. **308**, 60 (1998).
[20] D. Tripathi, T.K. Dey. J. Supercond. Nov. Magn. **28**, 2025 (2015).
[21] A. Arlina, S.A. Halim, M.M.A. Kechik, S.K. Chen. J. Alloys Compd. **645**, 269 (2015).
[22] E. Taylan Koparan, B. Savaskan, S.B. Guner, S. Celik. Appl. Phys. A **122**, 46 (2016).
[23] N.A. Kalanda, V.M. Trukhan, S.F. Marenkin. Inorg. Mater. **38**, 597 (2002).
[24] A.A. Bykov, K.Y. Terent'ev, D.M. Gokhfeld, N.E. Savitskaya, S.I. Popkov, M.I. Petrov. J. Supercond. Nov. Magn. **31**, 3867 (2018).
[25] M.I. Petrov, S.I. Popkov, K.Yu. Terentiev, A.D. Vasiliev. Pisma v ZhTF **46**, 11 (2020). (in Russian).
[26] M.I. Petrov, D.M. Gokhfeld, S.V. Semenov, I.V. Nemtsev. Pisma v ZhTF **50**, 11 (2024). (in Russian).
[27] D.M. Gokhfeld, M.I. Petrov, S.V. Semenov, A.D. Balaev, I.V. Nemtsev, A.D. Vasiliev, M.S. Molokeev. Ceram. Int. **50**, 52213 (2024).
[28] C. Changkang, A.T. Boothroyd, H. Yongle, F.R. Wondre, B.M. Wanklyn, J.W. Hodby. Phys. C Supercond. **214**, 231 (1993).
[29] K. Iida, N.H. Babu, Y. Shi, D.A. Cardwell. Supercond. Sci. Technol. **18**, 1421 (2005).
[30] V. Kuchárová, P. Diko, D. Volochová, V. Antal, M. Lojka, T. Hlásek, V. Plecháček. J. Eur. Ceram. Soc. **42**, 6533 (2022).
[31] A.D. Caplin, L.F. Cohen, M.N. Cuthbert, M. Dhalle, D. Lacey, G.K. Perkins, J.V. Thomas. IEEE Trans. Appiled Supercond. **5**, 1864 (1995).
[32] D.M. Gokhfeld. J. Supercond. Nov. Magn. **36**, 1089 (2023).
[33] D.M. Gokhfeld. Pisma v ZhTF **45**, 3 (2019). (in Russian).
[34] W. Guan, Y. Xu, S.R. Sheen, Y.C. Chen, J.Y.T. Wei, H.F. Lai, M.K. Wu, J.C. Ho. Phys. Rev. B **49**, 15993 (1994).
[35] D. Dew-Hughes. Philos. Mag. **30**, 293 (1974).
[36] H. Theuss, H. Kronmüller. Phys. C Supercond. Its Appl. **242**, 155 (1995).
[37] D.M. Gokhfeld, D.A. Balaev, I.S. Yakimov, M.I. Petrov, S.V. Semenov. Ceram. Int. **43**, 9985 (2017).
[38] D.M. Gokhfeld, S.V. Semenov, K.Y. Terentyev, I.S. Yakimov, D.A. Balaev. J. Supercond. Nov. Magn. **34**, 2537 (2021).
[39] G.S. Mkrtchyan, V.V. Shmidt. ZhETF, **61**, 367 (1972). (in Russian).
[40] J.R. Clem. *A Model for Flux Pinning in Superconductors, in Low Temperature Physics-LT 13* (Springer US, Boston, MA, 1974), pp. 102–106.
[41] F. Sernetz. J. Low Temp. Phys. **24**, 85 (1976).
[42] D. Gokhfeld. Phys. C Supercond. Its Appl. **619**, 1354486 (2024).

Translated by M.Verenikina